5 CURE CHARACTERISATION: DSC

This chapter looks at cure monitoring using differential scanning calorimetry (DSC). As the resin cures it will evolve the heat of reaction and this in principle can be used to monitor the progress of the reaction. Dynamic scans of the uncured material, using a heating ramp of 10°C min^{-1}, allowed the total heat of reaction (reaction enthalpy) to be calculated for each system. Isothermal scans of the uncured material were carried out by curing the material at a constant temperature within the sample chamber, and a running integral applied to the subsequent curve. Using the total heat of reaction, conversion curves could be plotted, allowing an activation energy to be calculated for each system. The isothermal scan durations were chosen to allow a return to a linear baseline after the maximum heat flow. Dynamic scans were then carried out on the isothermally cured samples to look at changes in the glass transition temperature.

The procedure followed has been summarised in the IUPAC Technical Report in 2006 [1]. The amount of material was adjusted so as to avoid the possibility of the exotherm leading to errors in the cure measurement. The cure of epoxy resins has been extensively investigated and the influence of changes in the structure of both the epoxy and amine quantified [2-7]. Significant changes in the rates of reaction and also the final values of the glass transition temperature are observed when either the epoxy or amine are changed from being aromatic to aliphatic-based reactants. The systems studied involve both aliphatic and aromatic-based materials.

5.1 STRATHCLYDE MODEL SYSTEM

Throughout this chapter, the samples were analysed under oxygen-free nitrogen, at 20 mL min^{-1}, and the heating/cooling rate was 10°C min^{-1}. The dynamic scans for the Strathclyde model system, shown in Figure 1, were integrated using the limits shown by the red lines. The scans had returned to linear baselines, although the second repeat scan was not particularly linear just before the peak. Integrating gave

values for the scans as 504.0 J g^{-1}, 515.4 J g^{-1} and 521.3 J g^{-1} respectively, with the average being 513.6 ± 7.2 J g^{-1}, where the error is the standard deviation. This value was taken to be the total heat of reaction for this particular system.

Isothermal scans on uncured samples were carried out at 35°C, 40°C, 45°C and 50°C (Figure 2). As the cure temperature was increased the maximum heat flow that each sample achieved increased, and the time to return to a linear baseline decreased. The isothermal curves can be seen to be asymmetric with a plateau region towards the maxima, particularly at higher cure temperatures. At the lower temperatures the epoxy resin will not have been completely cured and the matrix will still retain a certain amount of unreacted epoxy resin when the material becomes converted into the glass state. The reaction of poly-functional aliphatic amines has been observed to be auto catalytic and the activation energy changes with the degree of conversion [7]. The choice of the base line and the method used for the integration conforms with that proposed by the IUPAC document for recommending best practice in determination of cure [1].

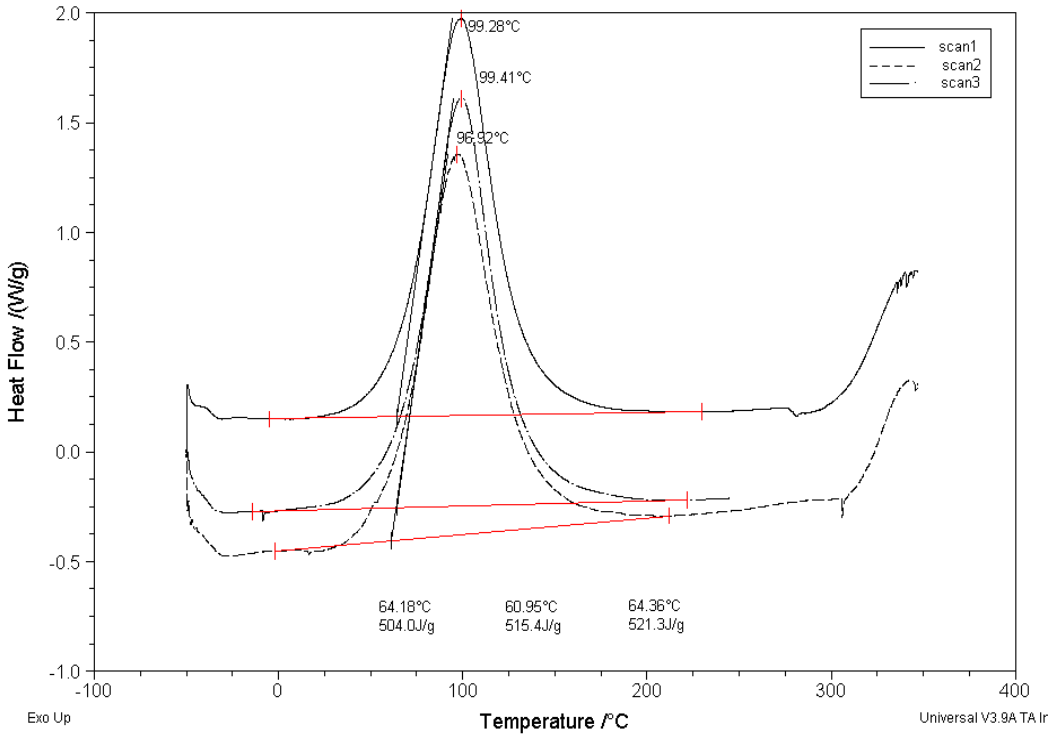

Figure 1. Dynamic DSC scan of uncured Strathclyde model system, showing how the heat flow varies with temperature.

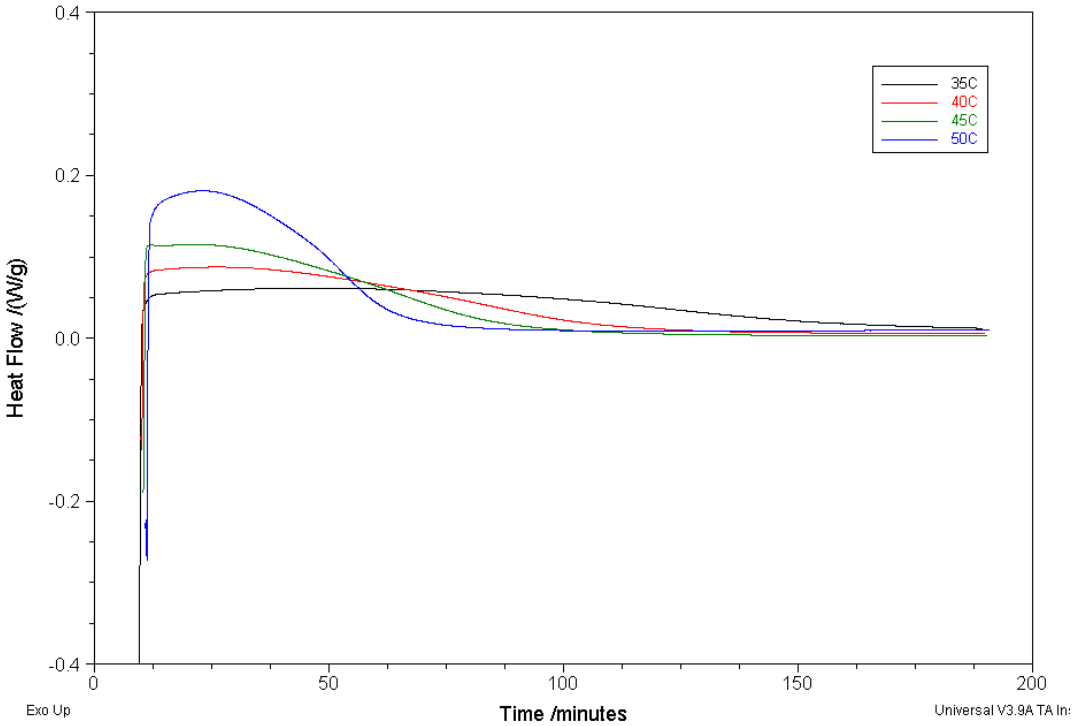

Figure 2. DSC scans of Strathclyde model system held isothermally, showing how the heat flow varies with the cure time.

The delay of *ca*. 10-12 minutes in Figure 2 before the response starts is due to the time taken for the samples to reach the programmed isothermal temperature, where the time at zero minutes is when the sample was first introduced to the DSC sample chamber. This occurred no more than five minutes after the epoxy and amine parts were mixed. The curves were integrated linearly, which gave a final integrated value for each one, as shown in Table 1.

Table 1. Final integral values of Strathclyde model system for the dynamic scan as well as for each isothermal scan.

Cure Temperature /°C	Final Integral Values /J g^{-1}
dynamic	513.6
35	307.2
40	331.4
45	357.0
50	394.6

The final integral values increased with increasing cure temperature, and they were all lower than the total heat calculated from the dynamic scan. A running integral

was applied to each integrated curve giving an integrated value every 0.5 minutes. Figure 3 shows the integrations applied to the 50°C sample, with the running integral shown in pink.

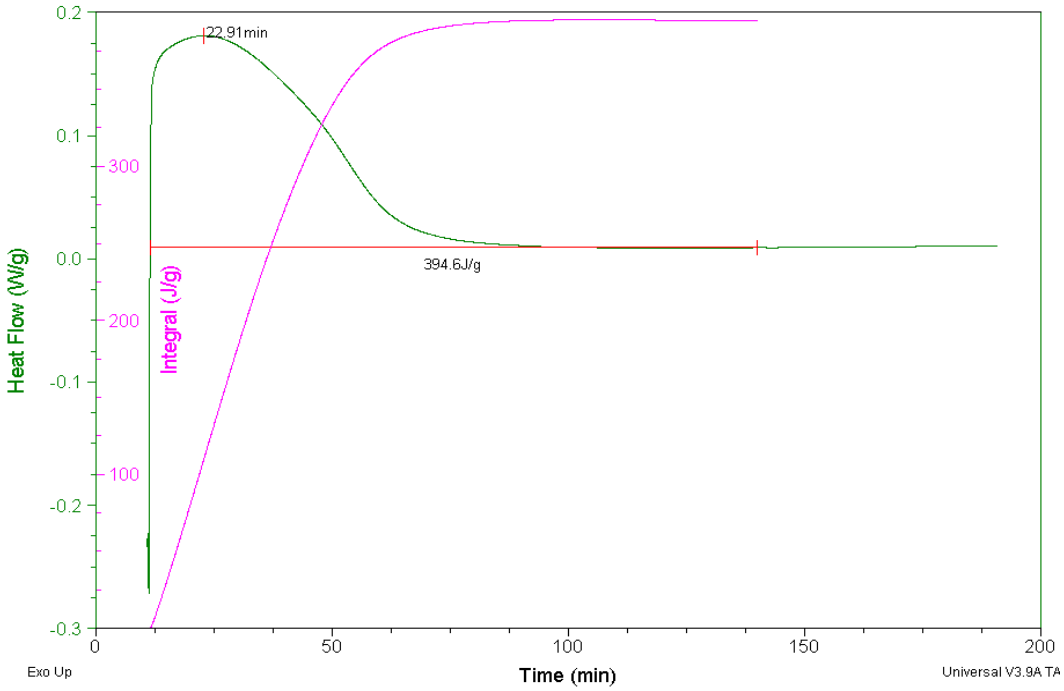

Figure 3. DSC isothermal curve of Strathclyde model system at 50°C - showing integration points, final integrated value (394.6 J g^{-1}), and the running integral (pink line).

The conversion curves were then plotted from the running integral values, with the time adjusted so that time zero was when the DSC first achieved the programmed isothermal temperature, as shown in Figure 4. It should be noted that the peak in the dynamic plot occurs at *ca.* 100°C and therefore it is not surprising that the cure carried out at temperatures that are up to 70°C lower than this optimum temperature are leading to lower degrees of final cure. In practice, resin cured at the lowest temperatures would require to be post cured in order to develop the optimum physical properties and achieve a satisfactory cured state.

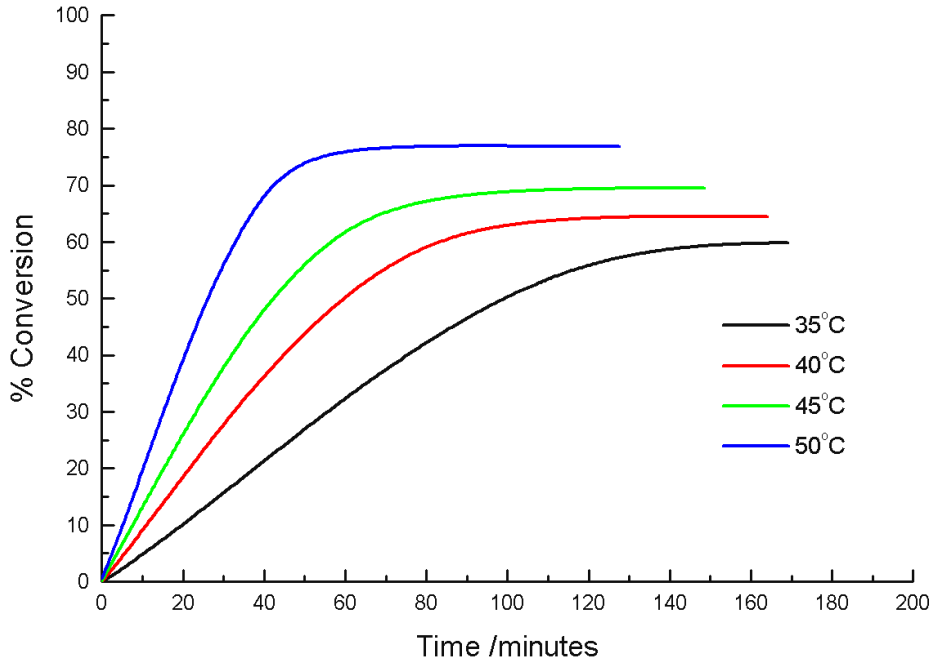

Figure 4. Conversion curves generated from the DSC data for the Strathclyde model system.

The conversion curves shown in Figure 4, were fitted using the Sigmoidal Boltzman equation in Origin - see Equation 1 below, where A_1 is the initial *y* value, A_2 is the final *y* value, x_0 is the centre (point of inflection) and dx is the width of the curve (the change in *x* corresponding to the most significant change in *y* values). The fitting function in Origin extrapolates the A_1 and A_2 values.

$$y = \frac{A_1 - A_2}{1 + e^{(x - x_0)/dx}} + A_2$$

Equation 1

The reaction rate was found for each isothermal cure temperature by taking the reciprocal of the dx value. Table 2 shows that as the cure temperature was increased the reaction rate and the final percentage conversion reached both increased.

Table 2. Final conversion values and rates of reaction calculated from the DSC data for the Strathclyde model system.

Cure Temperature /°C	Final % Conversion	Rate /min^{-1}
35	59.8	0.02958
40	64.5	0.04485
45	69.5	0.05467
50	76.8	0.08927

The rates observed in this study are comparable to those reported in the literature for aliphatic amine-cured systems [7]. Using the reaction rates, an Arrhenius plot was produced (Figure 5), and the activation energy was found to be: **58.1 kJ mol^{-1}**.

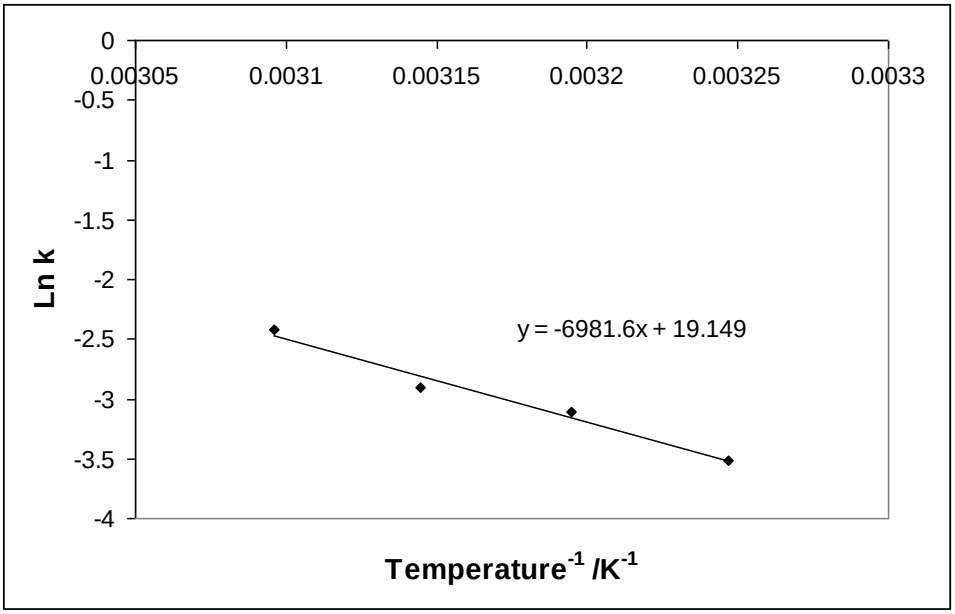

Figure 5. Arrhenius plot for the Strathclyde model system generated using DSC data.

Values of the activation energy for DEGBA cured with a branched chain polyamine have been reported to be *ca.* 56 kJ mol^{-1} which is comparable to that observed for this system [8-15]. Analysis of the changes in the rates of cure both with the degree of conversion and with temperature imply that the initial reaction involves the epoxy and primary amine, followed by secondary amine reaction being significantly slower. In this case, for a highly functionalised amine, once the degree of conversion exceeds *ca.* 30%, the process becomes diffusion controlled and ceases at *ca.* 80% conversion. The conversion plots reported for the polyamine are similar to those observed with this system. As the system becomes diffusion controlled the activation energy is observed to drop to a value of ~ 40 kJ mol^{-1}.

For the Strathclyde model system, each sample was held isothermally for 180 minutes and then a postcure dynamic scan was run at a heating rate of 10°C min^{-1}. Figure 6 shows that for each sample there is an enthalpic relaxation peak at approximately 50-75°C, followed by a much broader exothermic peak at

approximately 120°C that is due to further cross linking. It is likely that the enthalpic relaxation peak is masking the glass transition (T_g) step. There are various ways of using the software to calculate a value for comparison of the different samples including using the T_g calculation function, the peak area and using the value at the peak minima. However, it was felt that the on-set temperature of the peak is more closely related to the T_g than the peak minima or area, which are related to the enthalpic relaxation process, and is more accurate than using the T_g calculation function. The on-set temperature values are given in Table 3, and increase with increasing cure temperature.

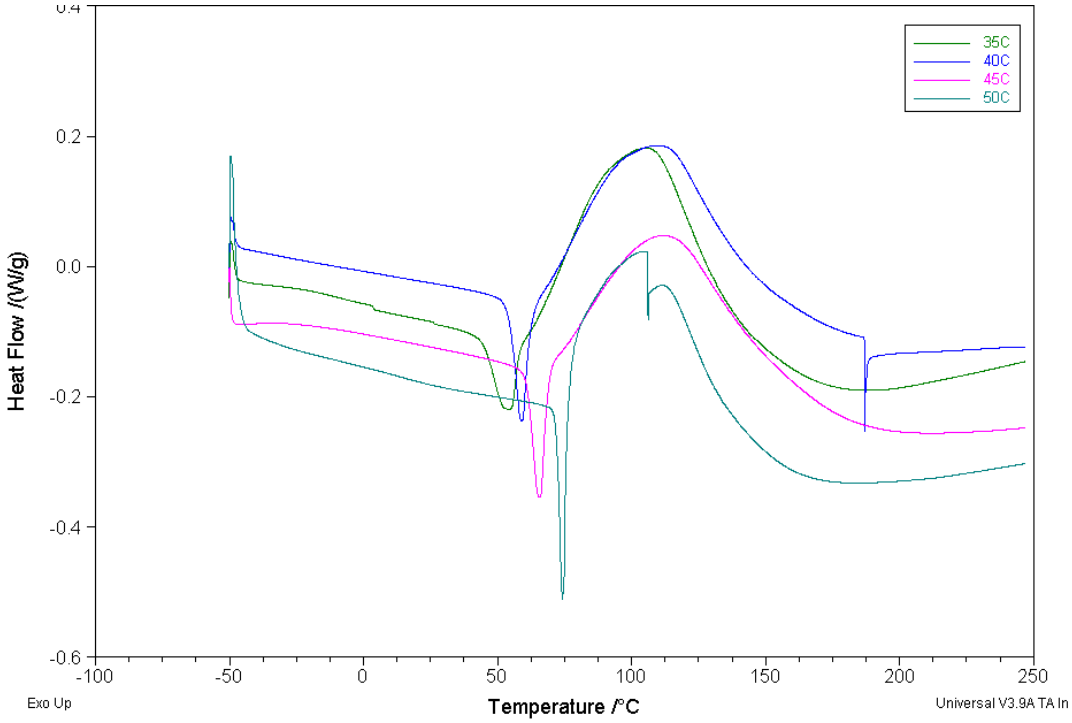

Figure 6. Postcure dynamic DSC scans of Strathclyde model system showing the change in heat flow as a function of temperature.

Table 3. Peak on-set temperature for the Strathclyde model system at each cure temperature.

Cure Temperature /°C	Peak On-set Temperature /°C
35	41
40	49
45	57
50	70

The cure process effectively ceases once the T_g has been reached and the DSC traces indicate that during post cure it is only when the T_g has been exceeded that reaction occurs. At the T_g stresses frozen into the resin during the conversion from a gel to a vitrified state would be expected to be released. This would in part account for the large amplitude of the negative peak that is rapidly reversed by the exotherm of the cure process. The trace for a fully cured system would normally consist of a small endothermic transition at T_g.

In the 35°C scan in Figure 6 two small deviations are seen at 3°C and 27°C, and are thought to be due to pan movement, possibly as a result of a small amount of ice build-up. The sharp peaks, seen above 100°C in the 40°C (at *ca.* 110°C) and 50°C (at *ca.* 180°C) scans, could be due to instrumental noise possibly as a result of a mains spike, or associated with the resin flow producing a better contact between the sample and the DSC pan. With the exception of the 50°C scan, a small kink can be seen between the enthalpic relaxation and the broad exotherm peak, e.g. for the 35°C scan it can be seen at *ca.* 62°C. This kink represents a separation in the T_g and the chemical process that gives way to the exotherm (further cross-linking as a result of postcuring).

It has been observed by a number of workers that determination of the T_g is difficult using DSC measurements [1, 4,7] and because of the nature of the exotherm associated with the enthalpic relaxation the value of the T_g is often significantly lower than that measured by other techniques.

5.2 SHARED MODEL SYSTEM

The dynamic scans shown in Figure 7 were integrated to give the total heats of reaction for scan1, scan2 and scan3 as: 465.5 J g^{-1}; 482.8 J g^{-1}; and 517.6 J g^{-1} respectively. The average total heat of reaction, and that used in subsequent calculations was 488.6 ± 21.7 J g^{-1}. This is comparable to that of the Strathclyde model system which had an average value of 513.6 ± 7.2 J g^{-1}.

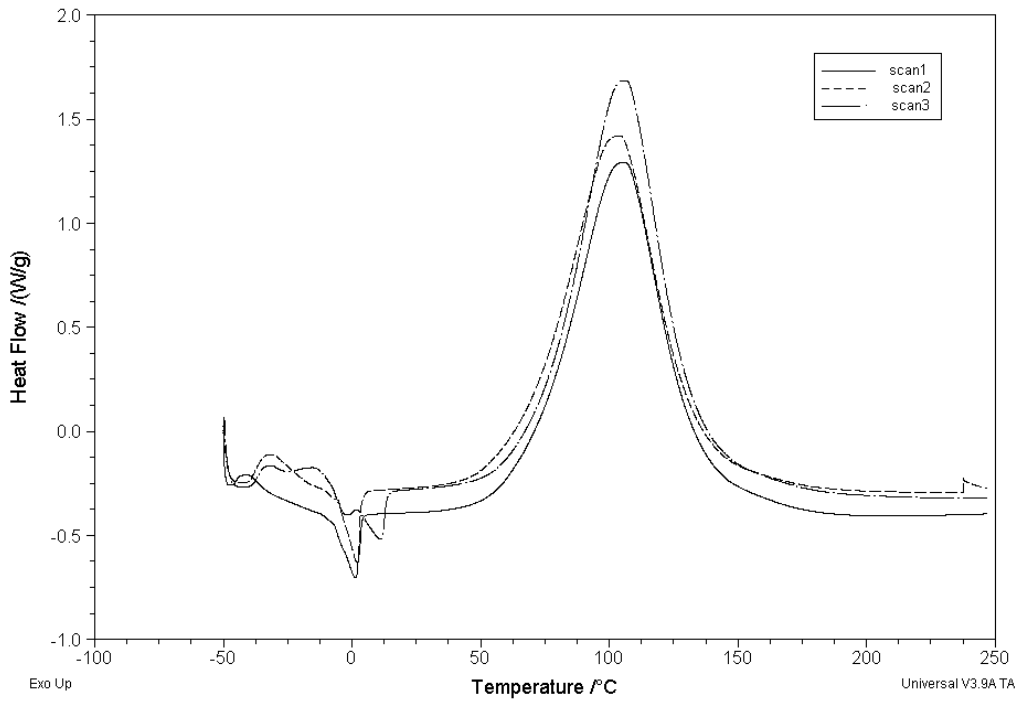

Figure 7. Dynamic DSC scans of shared model system, showing how the heat flow varies with temperature.

Isothermal scans on uncured samples were carried out at 45°C, 50°C, 55°C and 60°C (Figure 8). As the cure temperature was increased the maximum heat flow that each sample achieved increased, and the time to return to a linear baseline decreased. The curves are similar to the system with TETA in that they are asymmetrical, but have a slightly different shape as they do not have the same plateau region.

The curves were integrated linearly, which gave a final integrated value for each one, as shown in Table 4. The final integral values increased with increasing cure temperature, and they were all lower than the total heat calculated from the dynamic scan.

A running integral was applied to each integrated curve, as previously described, allowing the conversion curves to be plotted (Figure 9). The conversion curves were then fitted using the Sigmoidal Boltzman equation in Origin as previously described, and the reaction rate for each isothermal cure temperature was found.

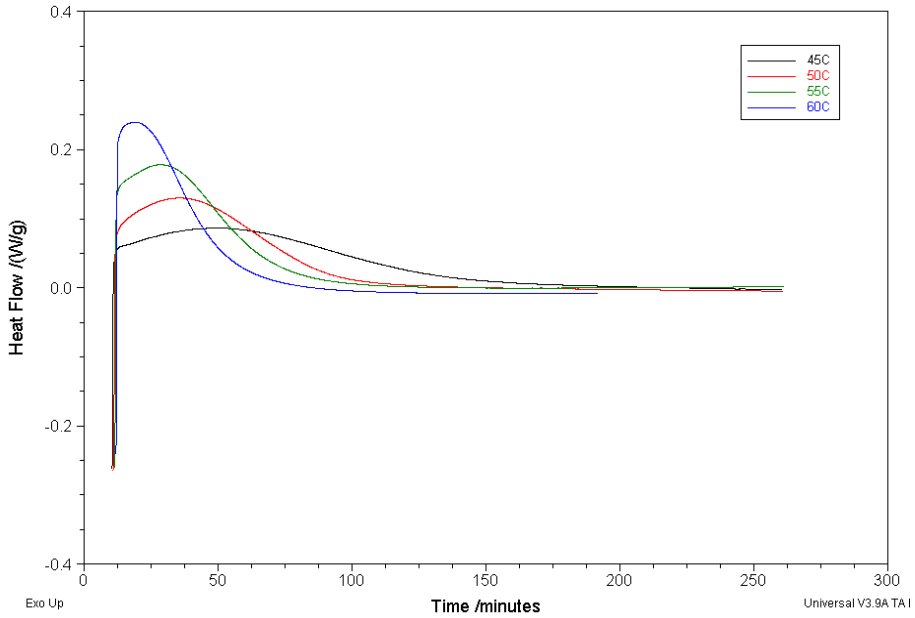

Figure 8. DSC scans of shared model system held isothermally, showing how the heat flow varies with the cure time.

Table 4. Final integral values of shared model system for the dynamic scan as well as for each isothermal scan.

Cure Temperature /°C	Final Integral Value /J g^{-1}
dynamic	488.6
45	484.7
50	462.9
55	448.0
60	436.3

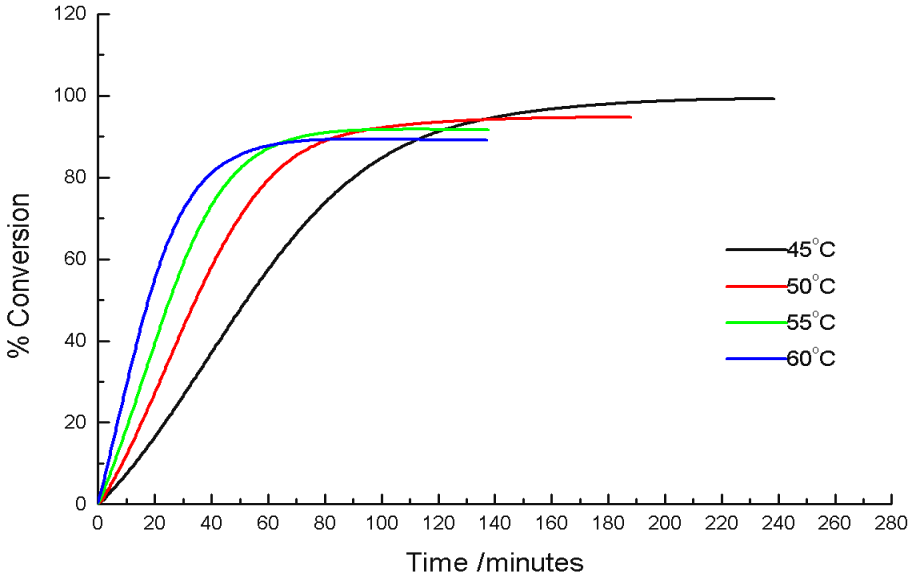

Figure 9. Conversion curves generated from the DSC data for shared model system.

Table 5 shows that as the cure temperature was increased the reaction rate increased. However, the final percentage decreased with cure temperature, instead of increasing as was shown in the case of the Strathclyde model system. This is due to the reactive groups becoming locked in place and not being able to react as a consequence of the cure schedule.

Table 5. Final conversion values and rates of reaction calculated from the DSC data for the shared model system.

Cure Temperature /°C	Final % Conversion	Rate /min^{-1}
45	99.2	0.03329
50	94.7	0.05437
55	91.7	0.07194
60	89.1	0.08290

It should be noted that with this system the extent of cure achieved even at the lowest temperature is significantly higher than that of the Strathclyde Model System. This reflects the lower density of crosslinking elements initially present in the system, i.e. the ratio of primary to secondary amine groups in the resin. At low temperatures reaction of the primary amine groups will be more facile than secondary groups with the consequential growth of linear chains rather than branched chain structures which are generated when secondary amine reactions contribute to the reaction. At the lower temperature a network is only formed when the degree of conversion has reached a high value. At higher temperatures the secondary amine reactions become more facile and a network, and hence glassy state, is created at lower degrees of conversion. The overall reaction scheme is complex and is a balance between the rate of the primary and secondary amine reactions [7].

Using the reaction rates, an Arrhenius plot was produced (Figure 10), and the activation energy was found to be: **53.3 kJ mol^{-1}.**

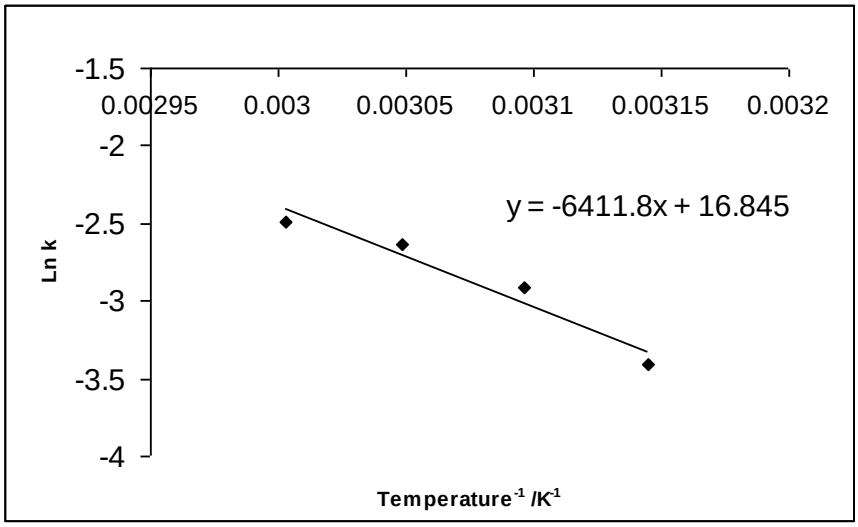

Figure 10. Arrhenius plot for the shared model system generated using DSC data.

Each sample was held isothermally for 250 minutes, apart from the 60°C sample which was only held for 200 minutes, before the postcure dynamic scan was run at a heating rate of 10°C min^{-1}. The resultant plots are shown in Figure 11.

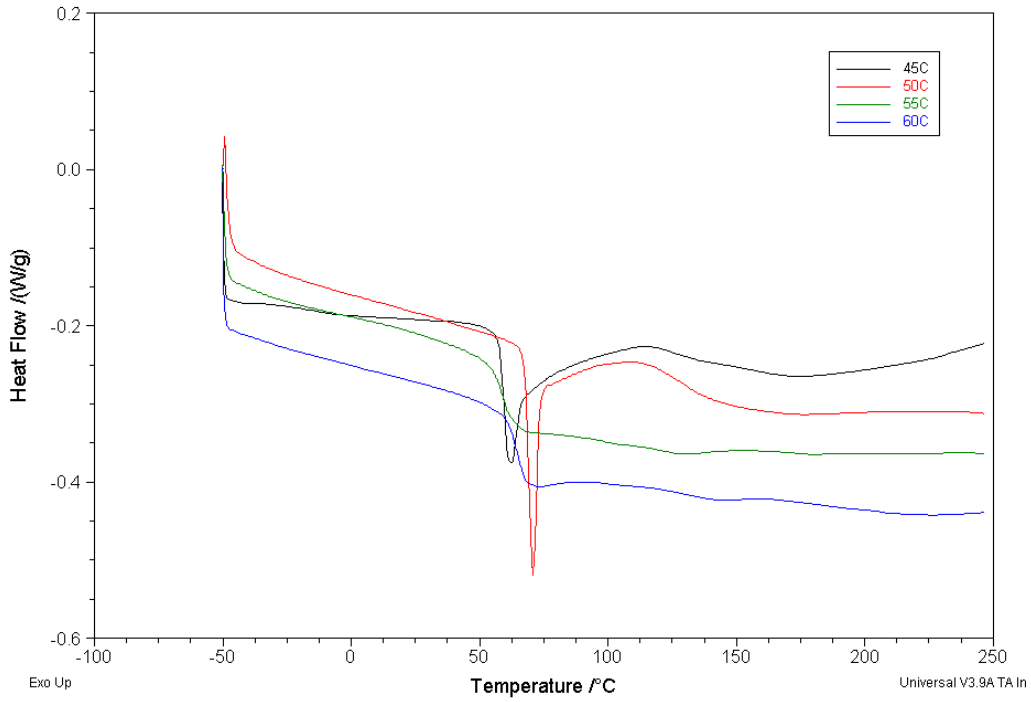

Figure 11. Postcure dynamic DSC scans of shared model system showing the change in heat flow as a function of temperature.

There is an enthalpic relaxation peak in the 45°C and 50°C scan, with a peak minimum at 63°C and 71°C respectively, followed by a much broader peak at 115°C and 109.39°C respectively. It is likely that the enthalpic relaxation peak is masking the glass transition (T_g) step in each case. For the 55°C and 60°C plots, a clear glass transition (T_g) step can be seen, and value is increased for the increased temperature. Table 6 shows the T_g values taken from the postcure scans. The peak on-set temperature was calculated for each cure temperature (Table 6), and for the 55°C and 60°C samples the difference between the peak on-set temperature and the calculated T_g was *ca.* 6°C. If the same difference were applied to the 45°C and 50°C scans, the T_g values would be *ca.* 61°C and 71°C which are both higher than expected.

Table 6. Peak on-set and T_g temperatures for the shared model system at each cure temperature.

Cure Temperature /°C	Peak On-set Temperature /°C	T_g /°C
45	55	-
50	65	-
55	54	60
60	59	65

As in the case of the Strathclyde model system the true values of the T_g are probably masked by the enthalpic relaxation of the matrix.

5.3 SK31

The dynamic scans shown in Figure 12 were integrated to give the total heats of reaction for scan1, scan2 and scan3 as: 129.9 J g^{-1}; 139.7 J g^{-1}; and 128.6 J g^{-1} respectively. The average total heat of reaction, and that used in subsequent calculation was 132.7 ± 6.1 J g^{-1}. This value is much lower than that of the Strathclyde and shared model systems which each had an average value of approximately 500 J g^{-1}. Isothermal scans on uncured samples were carried out at 25°C, 30°C, 35°C and 40°C (Figure 13). As the cure temperature was increased the maximum heat flow that each sample achieved increased, and the time to return to a

linear baseline decreased. The curves achieve a much lower maximum when compared to the two model systems, with a much broader peak.

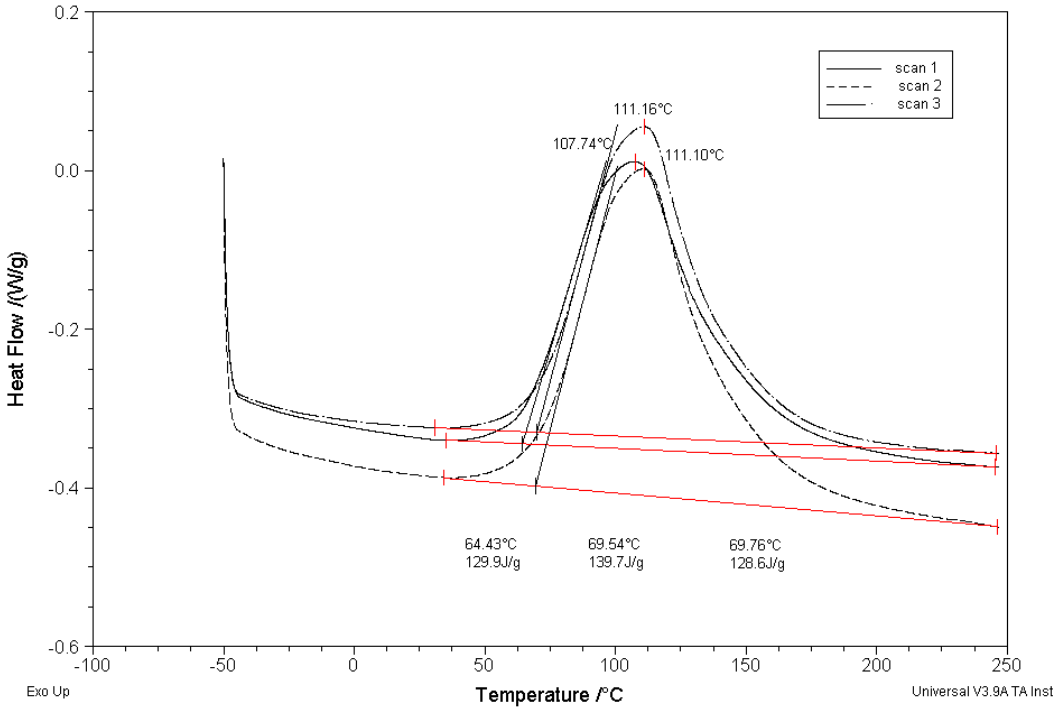

Figure 12. Dynamic DSC scans of SK31, showing how the heat flow varies with temperature.

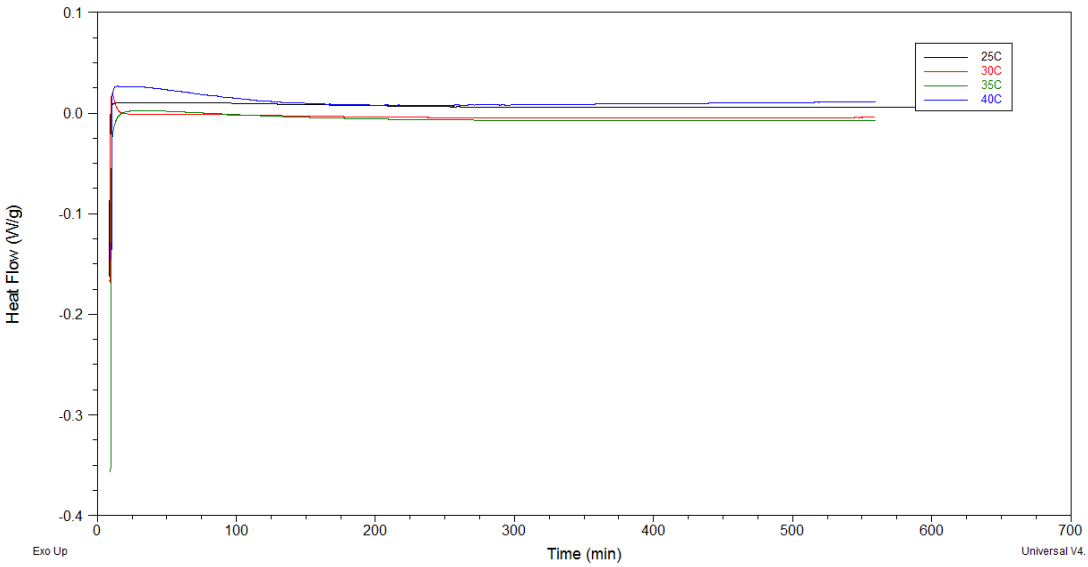

Figure 13. DSC scans of SK31 held isothermally, showing how the heat flow varies with the cure time.

The final integral values (Table 7) generally increased with increasing cure temperature, although the 30°C was lower than the 25°C value, and they were all lower than the total heat calculated from the dynamic scan. It should be noted that it was particularly difficult with this system to calculate the final integral values due to the shape of the curve and the difficulty in selecting the start and end points. It is likely that this has had an effect on the results reported below.

Table 7. Final integral values of SK31 for the dynamic scan as well as for each isothermal scan.

Cure Temperature /°C	Final Integral Value /J g^{-1}
dynamic	132.7
25	63.5
30	55.85
35	87.84
40	90.01

A running integral was applied to each integrated curve, as previously described, allowing the conversion curves to be plotted (Figure 14).

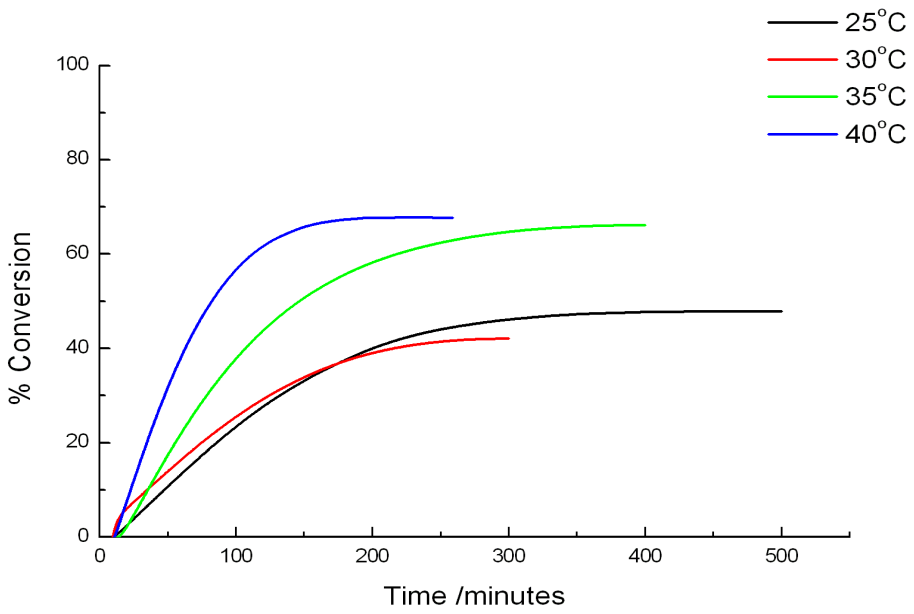

Figure 14. Conversion curves generated from the DSC data for SK31.

The conversion curves were then fitted using the Sigmoidal Boltzman equation in Origin as previously described, and the reaction rate for each isothermal cure

temperature was found. Table 8 shows that as the cure temperature was increased the reaction rate increased except for the 35°C where the value is much lower than expected due to the shape of the curve. The final percent conversion generally increased with increasing cure temperature, with the exception being for the 30°C cure and it was noted above that the final integral value for this sample was lower than expected.

Table 8. Final conversion values and rates of reaction calculated from the DSC data for SK31.

Cure Temperature /°C	Final % Conversion	Rate /min^{-1}
25	47.9	0.0138
30	42.1	0.0152
35	66.2	0.0136
40	67.7	0.0290

The reaction rates were used to produce an Arrhenius plot - when the 35°C rate was included within the plot the point lay below the fitted line and give an E_a of 32.4 kJ mol^{-1}. It was felt that this low rate value was a result of the applied integral limits being difficult to select resulting in a higher percent conversion and lower rate than would be expected. An Arrhenius plot excluding this data is shown (Figure 15) and the activation energy was found to be: **39.9 kJ mol^{-1}.**

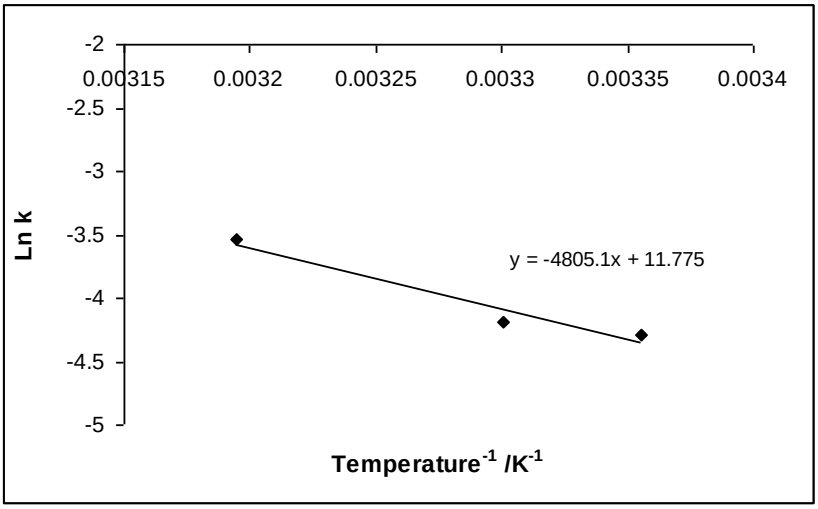

Figure 15. Arrhenius plot for SK31 generated using DSC data.

Each sample was held isothermally for 550 minutes, apart from the 25°C sample which was held for 600 minutes, before the postcure dynamic scan was run at a heating rate of 10°C min^{-1}. All four scans show a glass transition (T_g) step at approximately 30-50°C, and there is no enthalpic relaxation masking the T_g as noted for the two model systems. The calculated glass transition temperatures are given in Table 9, and show increasing T_g with increasing cure temperature.

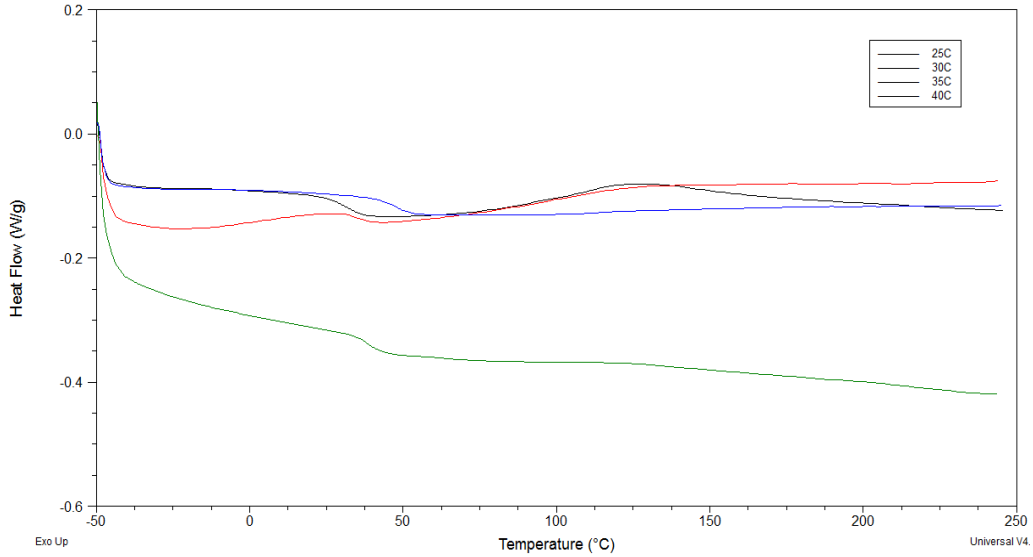

Figure 16. Postcure dynamic DSC scans of SK31 showing the change in heat flow as a function of temperature.

Table 9. Glass transition temperatures at each cure temperature - from postcure dynamic runs of SK31.

Cure Temperature /°C	T_g /°C
25	31
30	34
35	39
40	48

The values of T_g reflect the temperature used for the cure process and at typically 4-6°C above the cure temperature. The difference in the extent to which the value of the T_g is elevated is a reflection of the nature of the matrix which is being created and also nature of the reaction which is leading to the gelation and vitrification processes.

5.4 PR55

The dynamic scans shown in Figure 17 were integrated to give the total heats of reaction for scan1, scan2 and scan3 as: 359.0 J g^{-1}; 410.9 J g^{-1}; and 381.3 J g^{-1} respectively. The average total heat of reaction, and that used in subsequent calculation was 383.7 ± 21.3 J g^{-1}. This value is lower than that of the Strathclyde and shared model systems which each had an average value of approximately 500.0 J g^{-1}, but higher than that calculated for SK31 at 132.7 ± 6.1 J g^{-1}.

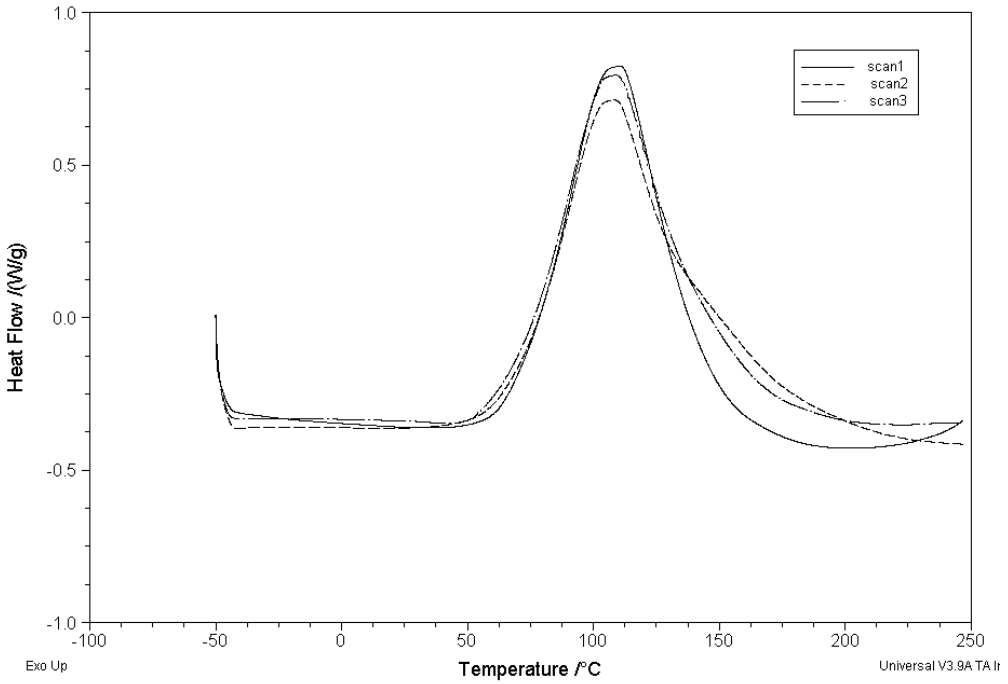

Figure 17. Dynamic DSC scans of PR55, showing how the heat flow varies with temperature.

Isothermal scans on uncured samples were carried out at 30°C, 35°C, 40°C and 45°C (Figure 18). As the cure temperature was increased the maximum heat flow that each sample achieved increased, and the time to return to a linear baseline decreased. The curves achieve a much lower maximum when compared to the two model systems, resulting in lower final integral values (Table 10). The final integral values generally increased with increasing cure temperature, and they were all lower than the total heat calculated from the dynamic scan. However, the final integral value for 40°C fell between those for 30°C and 35°C.

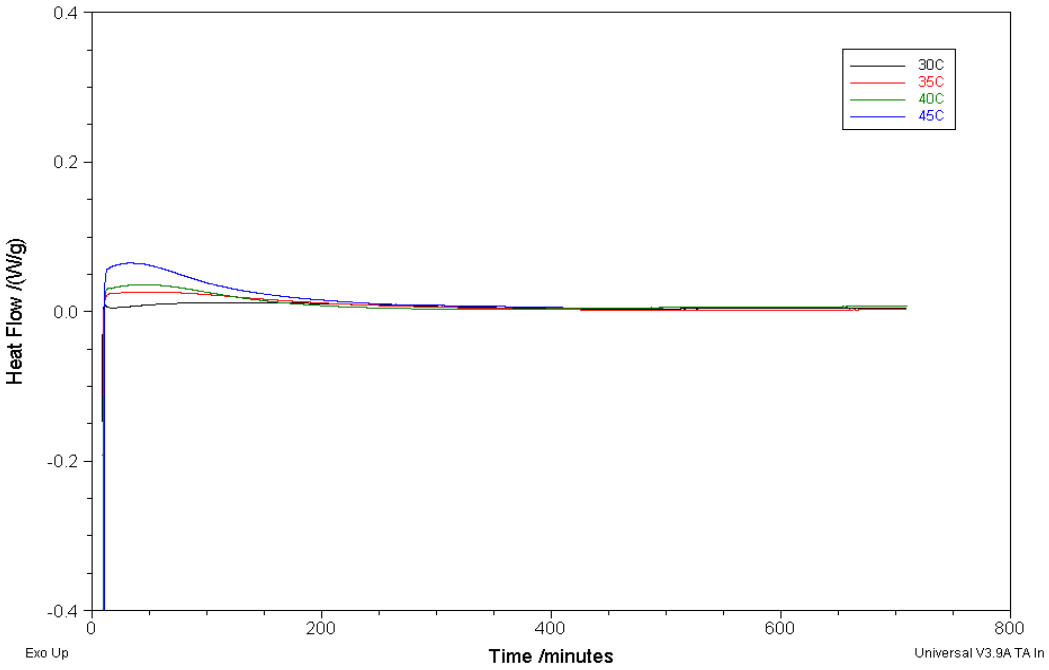

Figure 18. DSC scans of PR55 held isothermally, showing how the heat flow varies with the cure time.

Table 10. Final integral values of PR55 for the dynamic scan as well as for each isothermal scan.

Cure Temperature /°C	Final Integral Value /J g^{-1}
dynamic	383.7
30	116.4
35	270.4
40	249.1
45	321.6

A running integral was applied to each integrated curve, as previously described, allowing the conversion curves to be plotted (Figure 19). Figure 19 highlights the lower final integral value for the 40°C scan as it has a lower final conversion than the 35°C scan. The conversion curves were then fitted using the Sigmoidal Boltzman equation in Origin as previously described, and the reaction rate for each isothermal cure temperature was found - shown in Table 11 along with the final percentage conversion that each sample achieved. It can be seen, that while the 40°C final conversion was lower than that of the 35°C scan, the rates all increased with increasing cure temperature.

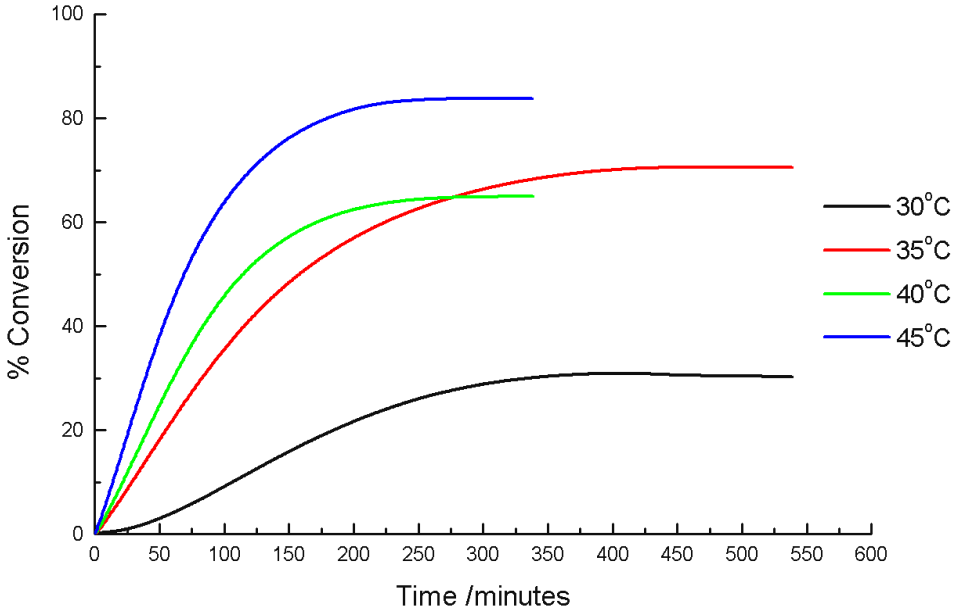

Figure 19. Conversion curves generated from the DSC data for PR55.

Table 11. Final conversion values and rates of reaction calculated from the DSC data for PR55.

Cure Temperature /°C	Final % Conversion	Rate /min^{-1}
30	30.3	0.00717
35	70.5	0.00858
40	64.9	0.01369
45	83.8	0.0153

As in the case of the shared model systems the degree of conversion for the isothermal plots shows different behaviour from that observed for the Strathclyde model system. As would be expected cure at 30°C shows a relatively low level of conversion and as the temperature is increased the degree of conversion is dramatically increased before showing the drop in values which is observed with the shared system.

Using the reaction rates, an Arrhenius plot was produced (Figure 20) and the activation energy calculated to be: **43.9 kJ mol^{-1}.**

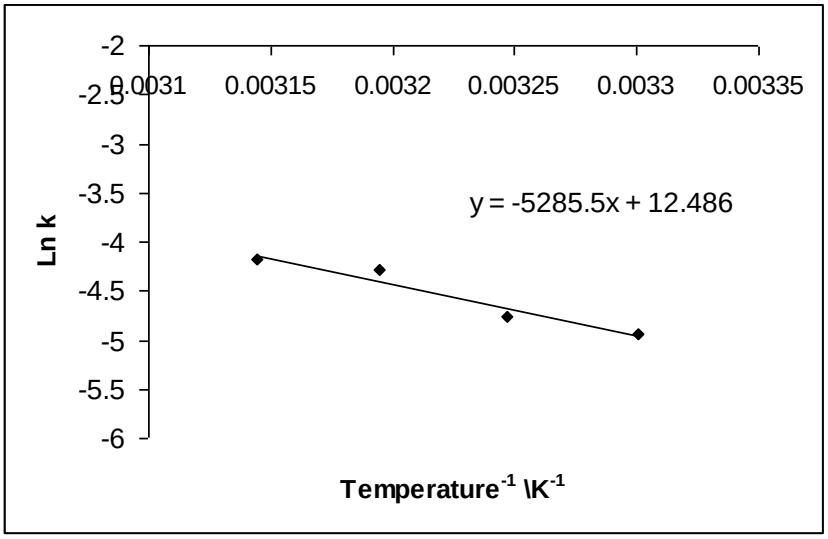

Figure 20. Arrhenius plot for PR55 generated using DSC data.

Each sample was held isothermally for 700 minutes, apart from the 45°C sample which was only held for 400 minutes, before the postcure dynamic scan was run at a heating rate of 10°C min^{-1}. The resultant plots are shown in Figure 21. As for the SK31 system, in most of the traces the T_g is easily identified and not masked by an enthalpic relaxation as was the case for the model systems.

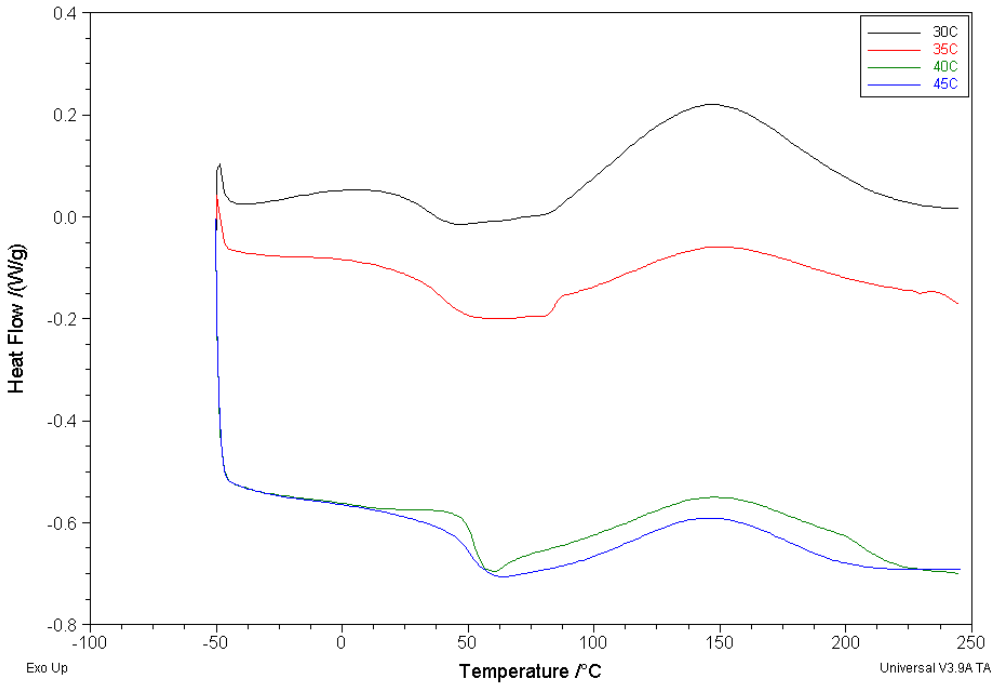

Figure 21. Postcure dynamic DSC scans of PR55 showing the change in heat flow as a function of temperature.

All four scans show a glass transition (T_g) step at approximately 30-50°C. The calculated glass transition temperatures are given in Table 12, and show increasing T_g with increasing cure temperature. It should be noted that compared to the 40°C sample, the other T_g processes are broader which would tend to indicate a heterogeneity and less well defined network. The apparent difference of the sample cured at 40°C was not investigated further.

Table 12. Glass transition temperatures at each cure temperature - from postcure dynamic runs of PR55.

Cure Temperature /°C	T_g /°C
30	33
35	40
40	52
45	51

The values of T_g reflect the temperature used for the cure process and at typically between 3 and 10°C above the cure temperature.

5.5 PRIME20

The dynamic scans shown in Figure 22 were integrated to give the total heats of reaction for scan1, scan2 and scan3 as: 470.0 J g^{-1}; 473.4 J g^{-1}; and 486.7 J g^{-1} respectively. The average total heat of reaction, and that used in subsequent calculation was 476.7 ± 7.2 J g^{-1}. This value is only slightly lower than that of the Strathclyde and shared model systems which each had an average value of approximately 500.0 J g^{-1}. For each scan, the baseline just before the peak was relatively linear with only scan3 proving more difficult to line up the first integration point. After the peak, it can be seen that all three scans had not quite returned to a completely linear baseline and the value at 250°C was used as the second integration point.

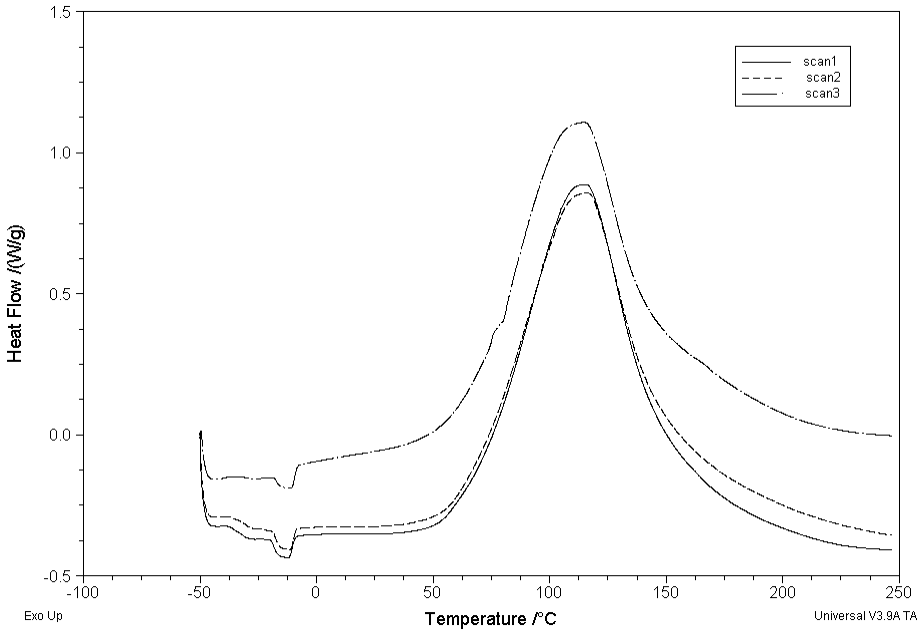

Figure 22. Dynamic DSC scans of Prime20, showing how the heat flow varies with temperature.

Isothermal scans on uncured samples were carried out at 40°C, 50°C, 60°C and 70°C (Figure 23). As the cure temperature was increased the maximum heat flow that each sample achieved increased, and the time to return to a linear baseline decreased. The curves achieved a much sharper maximum heat flow when compared to the previous systems studied.

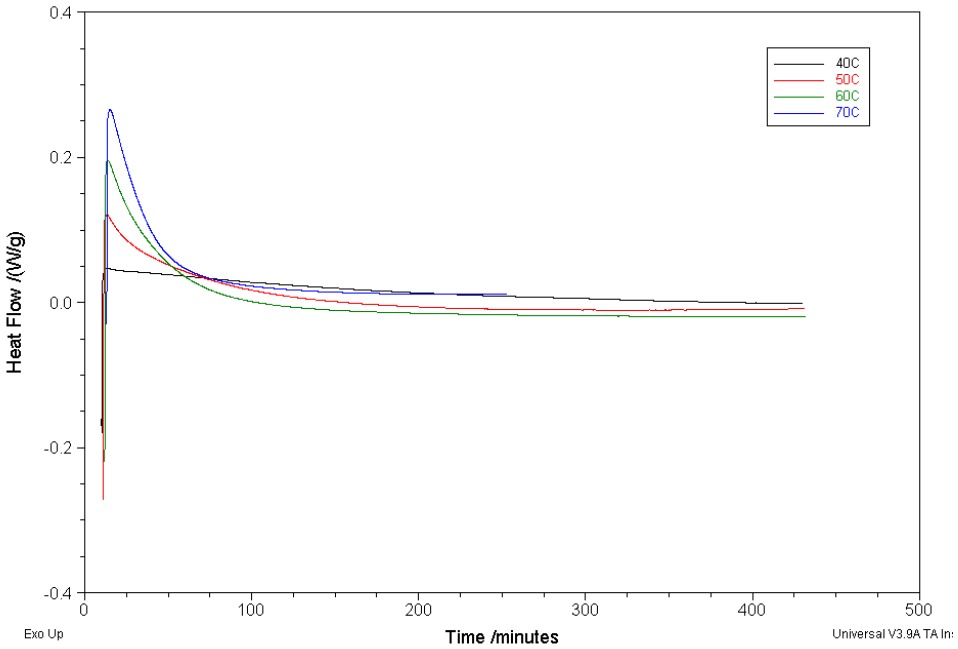

Figure 23. DSC scans of Prime20 held isothermally, showing how the heat flow varies with the cure time.

The final integral values increased with increasing cure temperature (Table 13), and they were all lower than the total heat calculated from the dynamic scan. The final integral values for 60°C and 70°C were very close, being 405.7 J g^{-1} and 407.6 J g^{-1} respectively.

Table 13. Final integral values of Prime20 for the dynamic scan as well as for each isothermal scan.

Cure Temperature /°C	Final Integral Value/ J g^{-1}
dynamic	476.7
40	367.7
50	373.8
60	405.7
70	407.6

A running integral was applied to each integrated curve, as previously described, allowing the conversion curves to be plotted (Figure 24). The conversion curves were then fitted using the Sigmoidal Boltzman equation in Origin as previously described, and the reaction rate for each isothermal cure temperature was found - shown in Table 14 along with the final percentage conversion that each sample achieved. It can be seen the rates all increased with increasing cure temperature.

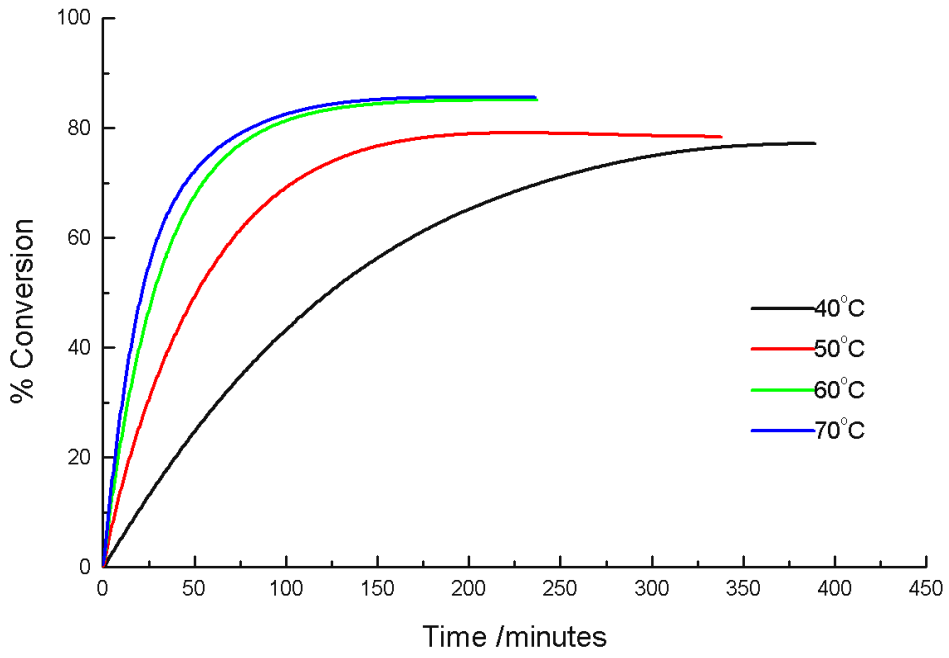

Figure 24. Conversion curves generated from the DSC data for Prime20.

Table 14. Final conversion values and rates of reaction calculated from the DSC data for Prime20.

Cure Temperature /°C	Final % Conversion	Rate /min^{-1}
40	77.1	0.00944
50	78.4	0.02063
60	85.1	0.03148
70	85.5	0.03726

Using the reaction rates, an Arrhenius plot (Figure 25) was produced and the activation energy calculated to be: **40.9 kJ mol^{-1}.**

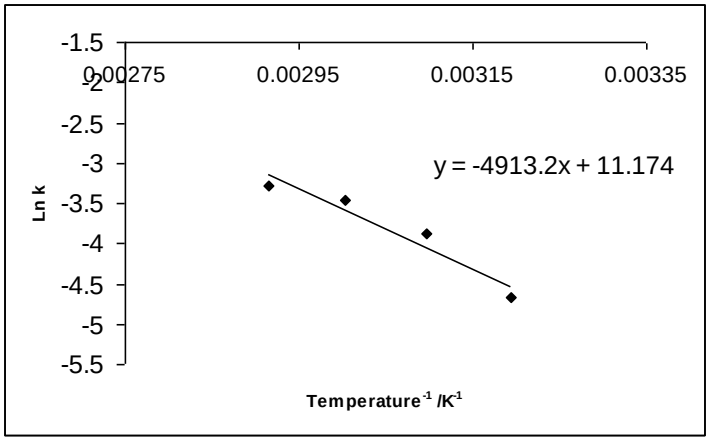

Figure 25. Arrhenius plot for Prime20 generated using DSC data.

Each sample was held isothermally for 420 minutes, apart from the 70°C sample which was only held for 250 minutes, before the postcure dynamic scan was run at a heating rate of 10°C min^{-1}. The resultant plots are shown in Figure 26. The scans at 40°C and 70°C show a clear glass transition (T_g) step at 50°C and 78°C respectively, as detailed in Table 15. The scans for 50°C and 60°C show an enthalpic relaxation which is masking the T_g. As with the other system studied the values of the T_g are higher than the temperatures used in the isothermal cure process.

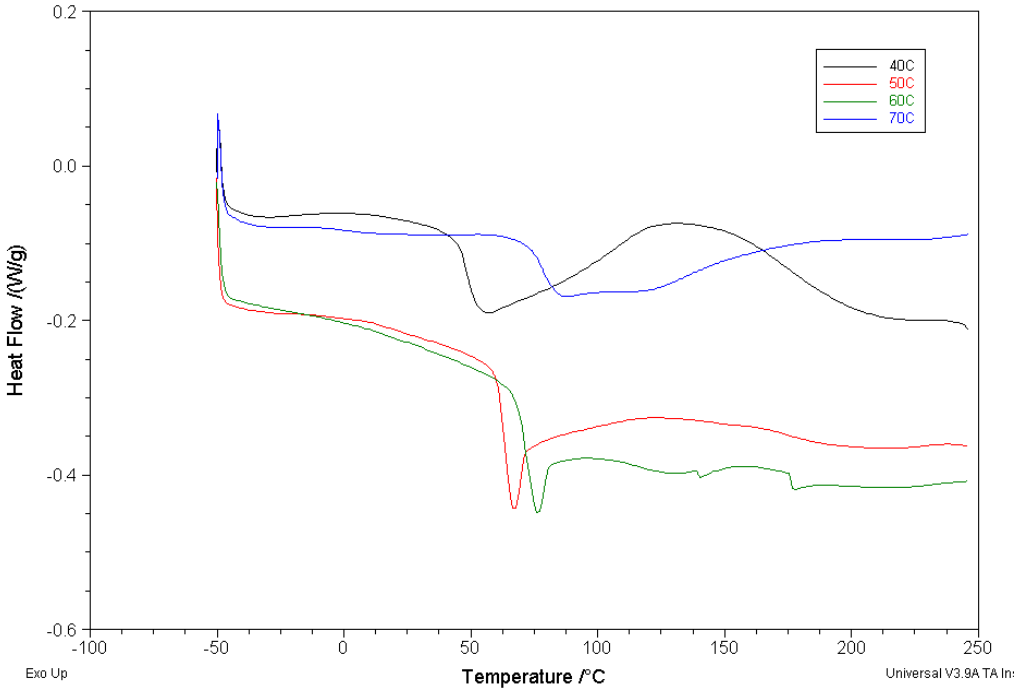

Figure 26. Postcure dynamic scans of Prime20 showing the change in heat flow as a function of temperature.

Table 15. Peak on-set and T_g temperatures at each cure temperature for Prime20.

Temperature /°C	Peak on-set Temperature /°C	T_g /°C
40	39	50
50	55	-
60	62	-
70	67	78

5.6 SP340

The dynamic scans shown in Figure 27 were integrated to give the total heats of reaction for scan1, scan2 and scan3 as: 296.2 J g^{-1}; 283.6 J g^{-1}; and 331.5 J g^{-1} respectively. The average total heat of reaction, and that used in subsequent calculation was 303.8 ± 20.3 J g^{-1}. This value is significantly lower than that of the Strathclyde and shared model systems which each had an average value of approximately 500.0 J g^{-1}. For each scan the baseline just before the peak was relatively linear. After the peak, it can be seen that all three scans had not quite

returned to a completely linear baseline and the value at 250°C was used as the second integration point.

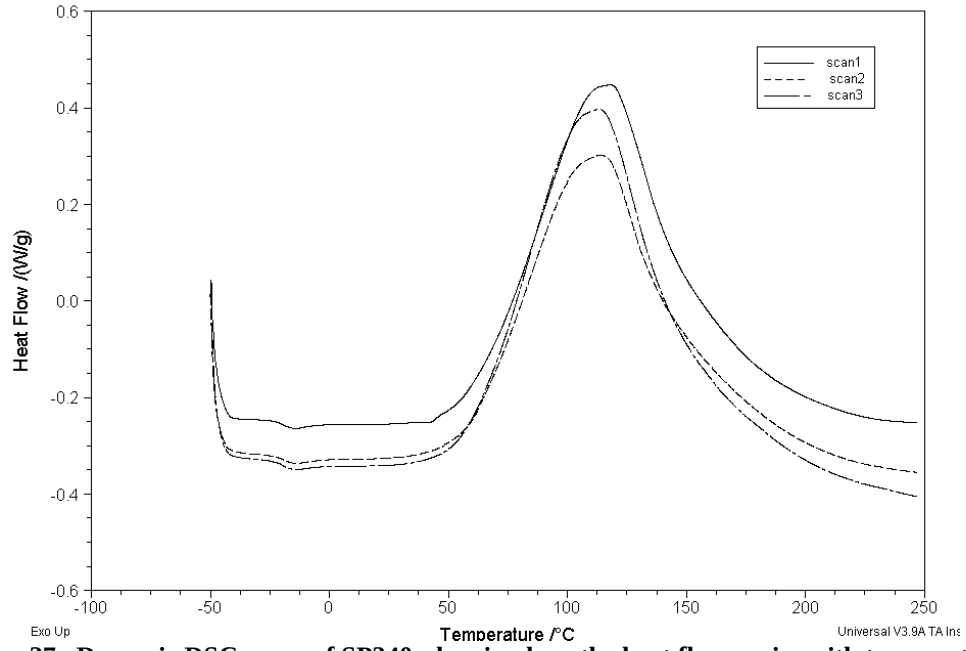

Figure 27. Dynamic DSC scans of SP340, showing how the heat flow varies with temperature.

Isothermal scans on uncured samples were carried out at 40°C, 50°C, 60°C and 70°C (Figure 28).

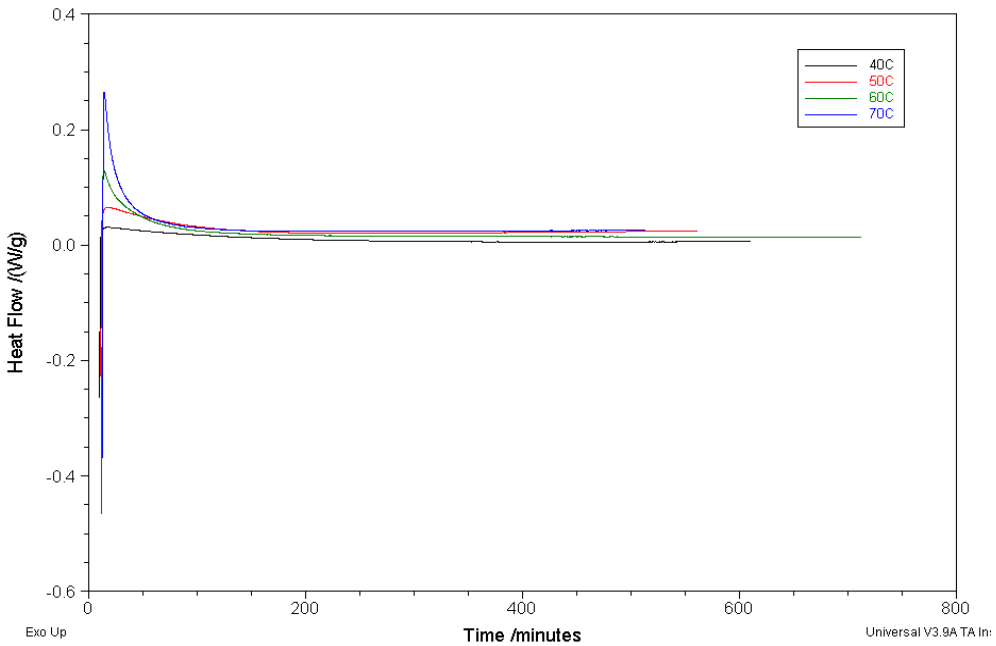

Figure 28. DSC scans of SP340 held isothermally, showing how the heat flow varies with the cure time.

As the cure temperature was increased the maximum heat flow that each sample achieved increased, and the time to return to a linear baseline decreased. The curves were similar to those produced for Prime20 and had a sharper maximum heat flow when compared to other previous systems studied. The final integral values increased with increasing cure temperature (Table 16), and they were all lower than the total heat calculated from the dynamic scan.

Table 16. Final integral values of SP340 for the dynamic scan as well as for each isothermal scan.

CureTemperature /°C	Final Integral Value /J g^{-1}
dynamic	303.8
40	156.2
50	164.8
60	219.0
70	236.6

A running integral was applied to each integrated curve, as previously described, allowing the conversion curves to be plotted (Figure 29). The conversion curves were then fitted using the Sigmoidal Boltzman equation in Origin as previously described, and the reaction rate for each isothermal cure temperature was found - shown in Table 17 along with the final percentage conversion that each sample achieved. It can be seen the rates all increased with increasing cure temperature.

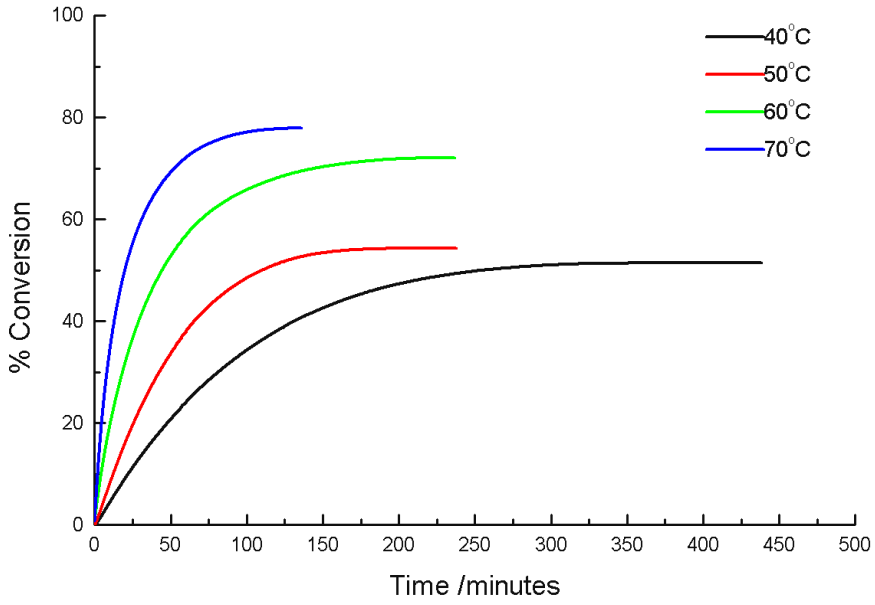

Figure 29. Conversion curves generated from the DSC data for SP340.

Table 17. Final conversion values and rates of reaction calculated from the DSC data for SP340.

Cure Temperature /°C	Final % Conversion	Rate /min^{-1}
40	51.4	0.01202
50	54.2	0.0219
60	72.1	0.02506
70	77.9	0.04524

Using the reaction rates, an Arrhenius plot (Figure 30) was produced and the activation energy calculated to be: **36.7 kJ mol^{-1}.**

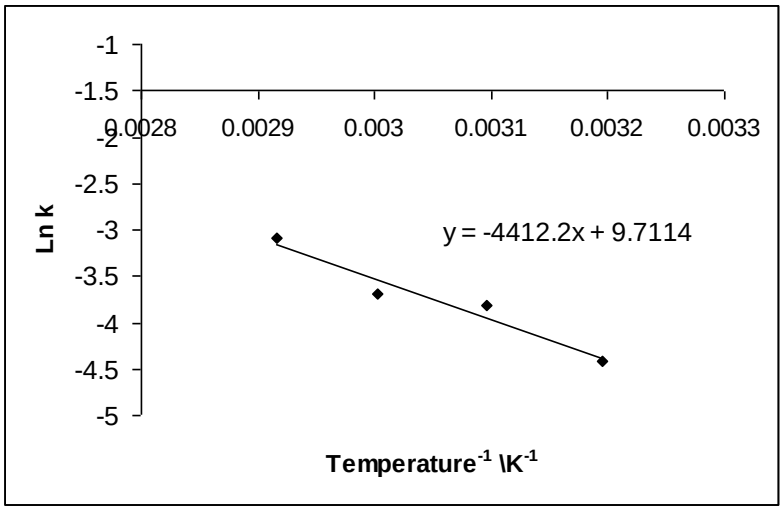

Figure 30. Arrhenius plot for SP340 generated using DSC data.

The samples were held isothermally at 40°C, 50°C, 60°C and 70°C, for 625 minutes, 575 minutes, 700 minutes and 500minutes respectively, before the postcure dynamic scan was run at a heating rate of 10°C min^{-1}. The resultant plots are shown in Figure 31. The scans all show a clear glass transition (T_g) step at approximately 40-70°C, as detailed in Table 18. The values of the T_g observed as with the other systems are all above the temperature used in the isothemal cure with the exception of the 70^{o}C cure where the value is essentially that same as that for the cure.

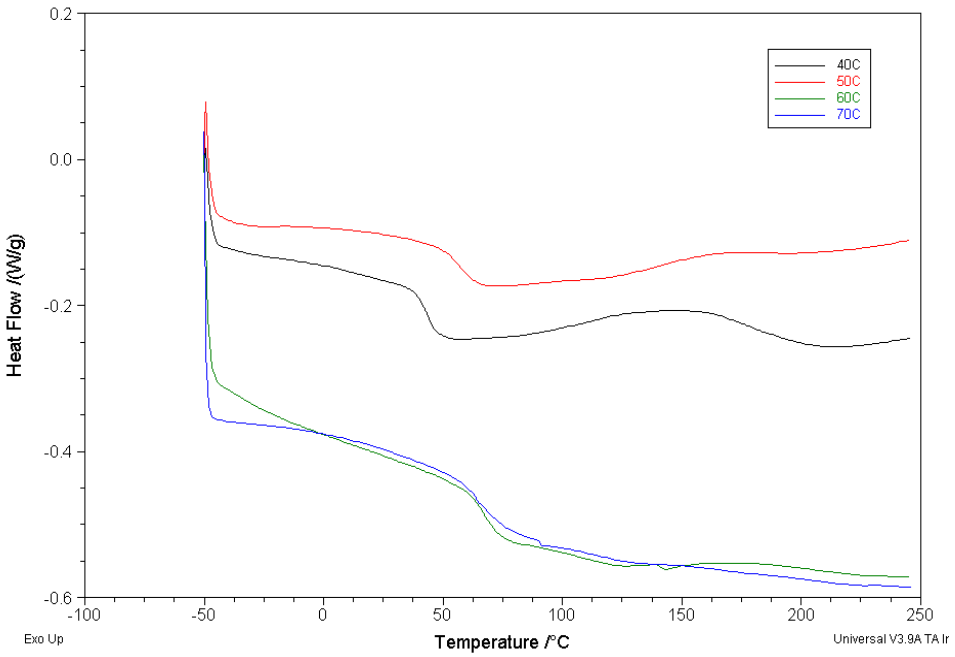

Figure 31. Postcure dynamic DSC scans of SP340 showing the change in heat flow as a function of temperature.

Table 18. Glass transition temperatures for each cure temperature from postcure dynamic runs of SP340.

Cure Temperature /°C	T_g /°C
40	42
50	55
60	67
70	68

5.7 CONCLUSIONS

In all the systems studied the initial cure does not lead to complete consumption of the epoxy resin during the cure process.

In the case of the Strathclyde system, which is based on the cure of triethylenetetramine the initial low temperature reaction will involve chain extension via the reaction of the primary amine groups. The linear polymer will gradually increase the viscosity and this will slow down the rate of reaction so that the system will slowly go through the gelation step and finally become vitrified. As the temperature is increased the rate for the reaction of the secondary reaction of the

amine becomes higher so that the chain will develop a branched chain structure. The branched chain will increase the viscosity less than the linear growing polymer with the effect that the mobility of the reactants will be retained to a higher extent than in the case of the linear growing chain. As a result the degree of conversion is increased by increasing the temperature. Despite the complexity of the reaction scheme as discussed in *Chapter 1* the system shows a simple Arrhenius type of rate plot which masks the detail of the reaction.

The principle difference between the Strathclyde model system and the shared model system is that the amine used (in the shared system) has two primary groups and no secondary groups. As a consequence the initial reactions have to lead to chain extension and it will be only relatively later in the reaction that the secondary reactions will become important. In this system, the two amine groups are linked by a highly flexible hexane group which will allow flexibility to be retained in the system until the network is finally formed in the vitrified state. The higher flexibility of the polymer chains which are formed allow a much higher degree of conversion to be achieved. The values of T_g are all very similar and reflect the flexibility of the hexane linkage and are lower than those for the Strathclyde model system.

The principle difference between SK31, a commercial system, and the two model systems is the addition, in this system, of the aliphatic-linked epoxy material (butanediol-diglycidyl ether) and the hindered amine. This system gave a much lower total heat of reaction compared to the model systems. The hindered amine leads, at lower temperatures, to the lower degrees of conversion.

PR55 is a commercial epoxy system in which the epoxy is a mixed resin system. The resin is formulated to balance rate of cure with viscosity allowing a faster reaction to be achieved at lower temperatures. The benzyl alcohol, at low temperatures, acts as a catalyst for the epoxy reaction and facilitates the reaction leading to an apparent lowering of the activation energy for the reaction. The reactivities of the aliphatic and aromatic-based epoxy resins are comparable but the aliphatic epoxy being more flexible leads to a lowering for the final T_g. The amine

being a cyclohexane ring system is significantly more hindered than the linear hexane structure used in the shared system and leads at lower temperatures to a low degree of conversion. Increasing the temperature leads to dramatic increase in the rate of reaction and the extent of conversion. Increasing the temperature will allow the cyclohexane ring to adopt a greater range of conformations and will facilitate the reaction with the epoxy groups.

Prime20 is a complex commercial system - the epoxy resin element of the system contains both the bisphenol A and F-based resins. The bisphenol-F epoxy tends to be less reactive than the bisphenol-A, but it has the advantageous effect of lowering the viscosity of the base resin system. The mobility of the base resin is further enhanced by the incorporation of the 1,4 butanediol diglycidyl ether which will promote the reaction at lower temperatures. The monofunctional aliphatic epoxy is used to plasticise the matrix. The trailing chain created by reaction of the mono function epoxy will introduce mobility into the matrix and increase its impact resistance. The amine component is similar to PR55 being based partly on isophoronediamine. The 2-piperazin-1-ylethylamine is a blend of primary and secondary amine groups that will favour an end capping reaction and suppress the viscosity build up in the initial stages. The phenol will act as a catalyst for the cure reaction and aid the lower temperature cure. Despite the complexity of the system the cure follows a simple reaction scheme and the extent of cure is weakly dependant on the cure temperature. The low activation energy for the process reflects the role of the phenol catalyst on the cure process.

SP340 is a commercial system with many constituents. The epoxy component is primarily composed of DGEBA, but also has a small amount of novolac resin that increases the viscosity of the uncured resin. The alkylgylcidylether, is a reactive diluent that is considered as a chain stopper as it reduces the functionality of the system, and hence the cross-linking is decreased. The hardener is a mostly flexible chain with a mix of other constituents. Benzyl alcohol and phenol are present as diluents which are plasticising in the presence of the isophoronediamine. This system has a relatively low activation energy compared to the other systems (likely

due to the phenol catalyst), but like the other systems follows a simple Arrhenius plot.

In summary, despite the complexity of the mixtures used the cure behaviour fits simple Arrhenius behaviour in all the systems studied. The rates of reaction reflect the changes in the composition of the mixture and the changes in blend of primary and secondary amine groups and more importantly the catalytic effect of the phenol groups on the reaction process.

5.8 REFERENCES

1. Gatta, G.D., M.J. Richardson, M. Sarges, and S. Stolen, *Standards, Calibration, and Guidelines in Microcalorimetry, Part 2*: *Calibration Standards for Differential Scanning Calorimetry*. Pure Appl. Chem, 2006. **78** (7): p. 1455–1476.

2. Hutchinson, J.M., F. Shiravand, Y Calventus, and I. Fraga., *Isothermal and non-isothermal cure of a tri-functional epoxy resin (TGAP): A stochastic TMDSC study*. Thermochimica Acta, 2012. **529**: p. 14–21.

3. Schawe, J.E.K., T. Hütter, C. Heitz, I. Alig, and D. Lellinger, *Stochastic temperature modulation: a new technique in temperature-modulated DSC*. Thermochim. Acta, 2006. **446**: p.147–155.

4. Zhang, J., Q. Guo, and B.L. Fox, *Study on thermoplastic-modified multifunctional epoxies: influence of heating rate on cure behaviour and phase separation.* Compos. Sci. Technol., 2009. **69**: p. 1172–1179.

5. Varley, R.J., J.H. Hodgkin, D.G. Hawthorne, and G.P. Simon, *Toughening of a trifunctional epoxy system. 2. Thermal characterization of epoxy/amine cure*. Journal of Applied Polymer. Science, 1996. **60**: p. 2251–2263.

6. Fraga I., S. Montserrat, and J.M. Hutchinson, *Vitrification and devitrification during the non-isothermal cure of a thermoset. Theoretical model and comparison with calorimetric experiments*. Macromol. Chem. Phys, 2010. **211**: p. 57–65.

7. Wana, J., Zhi-Yang Bu, Cun-Jin Xua, Bo-Geng Li, and Hong Fan, *Preparation, curing kinetics, and properties of a novel low-volatile starlike aliphatic-polyamine curing agent for epoxy resin.* Chemical Engineering Journal, 2011. **171**: p. 357–367.

8. Biju, R., C.P. Reghunadhan Nair, C. Gouri, and K.N. Ninan, *Rheokinetic cure characterization of epoxy–anhydride polymer system with shape memory characteristics.* J Thermal Analysis & Calorimetry, 2012. **107:** p. 693–702.

9. Rabearison, N., C. Jochum, and J.C. Grandidier, *A cure kinetics, diffusion controlled and temperature dependent, identification of the Araldite LY556 epoxy*. J Materials Science, 2011. **46**: p. 787–796.

10. Tan, S.G., and W.S. Chow, *Thermal properties of anhydride-cured bio-based epoxy blends.* J Thermal Analysis & Calorimitry, 2010. **101**: p. 1051–1058.

11. Musto, P., M. Abbate, G. Ragosta, and G. Scarinzi, *A study by Raman, near-infrared and dynamic-mechanical spectroscopies on the curing behaviour, molecular structure and viscoelastic properties of epoxy/anhydride networks.* Polymer, 2007. **48**: p. 3703-3716.

12. Liu, Y., Z. Du, C. Zhang, C. Li, and H.Li, *Curing Behavior and Thermal Properties of Multifunctional Epoxy Resin with Methylhexahydrophthalic Anhydride*. Journal of Applied Polymer Science, 2007. **103**: p. 2041–2048.

13. Floresa, M., X. Fernández-Francos, X. Ramis, and A. Serra, *Novel epoxy-anhydride thermosets modified with a hyperbranched polyester as toughness enhancer. I. Kinetics study*. Thermochimica Acta, 2012. **544:** p. 17–26.

14. Xu, J., M. Holst., M. Wenzel and I. Alig, *Calorimetric Studies on an Anhydride-Cured Epoxy Resin from Diglycidyl Ether of Bisphenol-A and Diglycidyl Ether of Poly(propylene glycol). I. Onset of Diffusion Control During Isothermal Polymerization*. Journal of Polymer Science: Part B: Polymer Physics, 2008. **46:** p. 2155–2165.

15. Harsch, M., J. Karger-Kocsis, and M. Holst, *Influence of fillers and additives on the cure kinetics of an epoxy/anhydride resin*. European Polymer Journal, 2007. **43**: p. 1168 -1178.